

## 3D printing of functional metallic microstructures and its implementation in electrothermal actuators

O. Fogel<sup>a,b,\*</sup>, S. Winter<sup>a</sup>, E. Benjamin<sup>c</sup>, S. Krylov<sup>c</sup>, Z. Kotler<sup>a</sup>, Z. Zalevsky<sup>b</sup>

<sup>a</sup> Additive Manufacturing Lab, Orbotech Ltd., P.O. Box 215, Yavne 81101, Israel

<sup>b</sup> Faculty of Engineering and the Nanotechnology Center, Bar Ilan University, Ramat-Gan, 52900, Israel

<sup>c</sup> School of Mechanical Engineering, Faculty of Engineering, Tel Aviv University, Ramat Aviv 6997801, Israel

### ARTICLE INFO

#### Keywords:

LIFT  
3D printing  
Thermal actuator  
Laser induced forward transfer  
MEMS

### ABSTRACT

Laser-induced forward transfer (LIFT), a 3D Pleaadditive manufacturing technique is implemented to fabricate a fully metallic functional micro device. Digital deposition of both structural and sacrificial metal constituents in the same setup arrangement is achieved. The final free-standing structure is released by selective chemical wet etching of the support material. Using this approach, a chevron-type electro thermal micro-actuator made of gold was successfully fabricated and its functionality was shown in experiment. Comparison of the measured responses with the model predictions indicates that the thermal conductivity of printed Au is approximately 8 times lower than the bulk value. It is a first demonstration of a functional micron scale actuator printed using LIFT.

### 1. Introduction

3D printing is becoming increasingly widespread with the emergence of new applications demonstrating advantages of additive manufacturing over conventional fabrication methods, for example, printing of hybrid structures [1,2], printing on flexible substrates [3,4] and building complex geometries [5,6]. Among functional materials, metals are of great interest due to their mechanical, electrical and thermal properties, which allow for a wide range of functional structures and devices to be manufactured. Common metal printing methods are usually of limited resolution (larger than 50  $\mu\text{m}$ ), which render them less relevant for manufacturing of micro devices. Ink and paste based printing methods have the additional disadvantage of requiring post-printing sintering process in order to remove the organic material. Additionally, printing of inks is strongly dependent on the wetting properties of the substrate by the droplets. In the realm of microelectromechanical systems (MEMS) the lithography based fabrication approaches are essentially planar. While printing of complex 3D micro and nano structures, such as nanophotonic or acoustic meta materials [7], was demonstrated, mainly polymeric electrically non-conductive materials were used. As a result, these structures cannot be directly implemented as functional actuators. A recent study has shown micron-scale Ni structures built by two-photon lithography using hybrid organic–inorganic materials containing Ni clusters [8]. A review of micron-scale metal printing methods was recently published by Hirt et al.

[9].

Laser induced forward transfer (LIFT) is a printing method which enables the deposition of a wide range of materials including metals in their bulk form. In this method, a pulsed laser is focused on the interface of a transparent substrate coated with the desired metal, referred to as the donor. Under the right combination of pulse duration and energy and of the donor thickness, each laser pulse gives rise to jetting of a single metal droplet. This printing technique was shown to demonstrate high resolutions (less than 20  $\mu\text{m}$ ), does not require post-treatment and allows for the buildup of high aspect ratio structures [10,11]. Because of the large variety of metals that can be deposited by LIFT under similar printing conditions, multi-metal structures can be fabricated with relative ease. Some studies [10,12,13] have shown examples of 3D LIFT printed structures, however LIFT printed MEMS actuators have yet to be demonstrated.

The electrical properties of LIFT printed metals, specifically printed copper and aluminum [14–16], have been studied in order to validate their applicability for digital manufacturing of electrical circuitry. It was shown previously that LIFT printed copper and aluminum structures suffer from the presence of nanometric voids and consequently porosity as well as from oxidation of the metal drops during deposition, all affecting the eventual electrical properties of the material. The effect of the partial oxidation of the molten droplets as they travel toward the acceptor substrate can be avoided by carrying out the printing process under non-oxidizing atmosphere [11,15]. In addition, a LIFT printed Pt-

\* Corresponding author at: Additive Manufacturing Lab, Orbotech Ltd., P.O. Box 215, Yavne, 81101, Israel.  
E-mail address: [ofer-fo@orbotech.com](mailto:ofer-fo@orbotech.com) (O. Fogel).

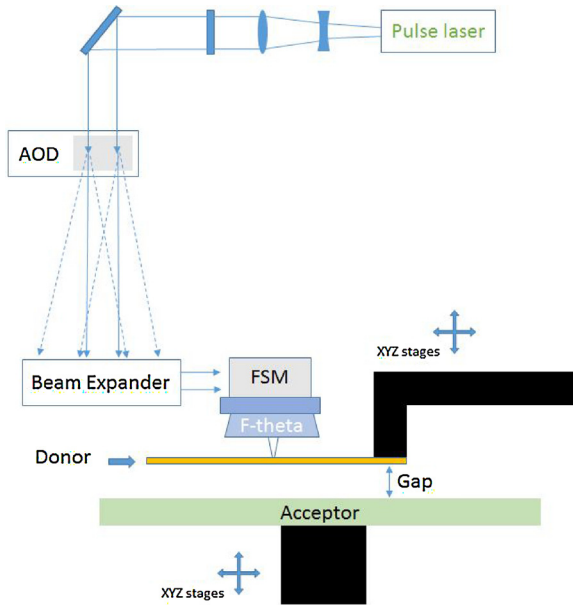


Fig. 1. LIFT setup.

Au thermocouple has shown Seebeck coefficient lower than bulk [17]. While the electrical properties of LIFT printed metals were the subject of several studies, mechanical and thermal properties have been much less researched. When considering fabrication of micrometer-scale mechanical devices, such as MEMS actuators, the mechanical properties of LIFT printed structures are of the highest interest.

In this work, we report on fabrication and characterization of a LIFT printed chevron-type electro thermal actuator, which, to the best of our knowledge, is the first demonstration of a 3D printed functional fully metallic micrometer scale actuator. We find that the thermal conductivity of printed Au is 8 times lower than that of bulk Au. This demonstrates the capacity to LIFT print complex and multi-material functional MEMS devices.

## 2. Materials and methods

Fig. 1 depicts the LIFT setup used for printing. A laser with a pulse duration of 0.8 ns and a wavelength of 532 nm (Picospark (3W), Teem Photonics) is used for the LIFT process. A Gaussian spot with a fixed spot size of  $\approx 28 \mu \pm 0.5 \mu \text{m}$  (4-sigma) at the donor interface was used in these experiments. The spot is scanned using an acousto-optical scanner (AOD) and a galvanometer scanner allowing various shape patterns to be conveniently printed. The AOD also serves to control the pulse energy. The donor and the acceptor are each positioned on xyz translation stages and are held in place by vacuum holders. The donor holder supports two slides allowing printing structures composed of two different materials in a rather convenient manner. The metal layers (either Cu or Au) were sputter deposited on glass slides with a typical thickness of 500 nm were the suitable donor, coated with the required printing metal, was loaded before the printing. The cantilever beams samples were printed on a sheet of FR4 laminate.

The printing algorithm we used is described by Zenou et al. [12]. In order to build the pattern in height, several layers were printed until the desired thickness was achieved. In this printing algorithm each layer consists of dividing the required pattern into  $N$  matrices, and the donor is moved to a fresh spot between each matrix. The space between two adjacent jettings within each matrix is larger than the heat affected zone of a single jetting. In our study, we used  $35 \mu \text{m}$  spacing between adjacent jettings and each layer consisted of 64 matrices.

In order to maintain the space between the donor and the printed structure in the range between  $200 \mu \text{m}$  and up to  $300 \mu \text{m}$ , according to

the structure building progress, the acceptor stage was moved (as described in the printing process section).

In this work LIFT printed complex shape 3D structure fabricated by combining a sacrificial metal along with a structural metal [15]. Both metal types (sacrificial and structural) are printed using the same laser setup and under similar printing conditions. We used Au as the structural material for the fabrication of the actuator while Cu was printed as the sacrificial layers.

## 3. Results and discussion

### 3.1. LIFT printed actuator

To print 3D complex structure, sacrificial structure was printed using Cu coated glass slides (as described in Section 2). The laser pulse energy for Cu printing was  $5.5 \mu \text{J}$  and the space between the donor and the acceptor was set to  $300 \mu \text{m}$ . The sacrificial structure was a trapezoid where the base was a  $3.6 \text{ mm} \times 0.4 \text{ mm}$  rectangle with  $3.4 \text{ mm} \times 0.4 \text{ mm}$  rectangle on top, with a total thickness of  $\approx 95 \mu \text{m}$  (10 layers). Following the Cu printing, the acceptor stage was moved down to verify that the gap (the space between the top of the sacrificial structure to the donor) was  $300 \mu \text{m}$ . An Au coated glass slide was used for printing the V-shape beam and pads. For the Au printing a pulse energy of  $4.25 \mu \text{J}$  was used to build  $50 \mu \text{m}$  thickness (5 layers) of Au.

After completion of the printing a chemical wet etch process is used to selectively remove the sacrificial material. Specifically, a FeCl (30%) solution served to selectively etch the printed Cu structure. Fig. 2 (a)-(c) depicts SEM images of the printed actuator structure before and after etching. Using this technique, a thermal actuator composite of two straight beams which create a chevron shape was printed. The geometric parameters of the device are detailed in Table 1.

### 3.2. Model

To evaluate the design parameters and estimate the expected performance of the actuator a reduced order (lumped) model of the device was built. Various approaches were reported for the analysis of V-shaped electro thermal micro actuators, starting from simple truss models [18,19] and up to nonlinear beam theories valid for large deflections [20–22]. In the present work we describe the device in the framework of the double clamped weakly nonlinear shallow Euler-Bernoulli beam theory, which is well-established and widely used for the modeling of micro scale structures [23]. The deflections  $w(x)$  of the beam satisfy to the equilibrium equation

$$EI_{yy}w'''' + \left( EA\alpha\bar{\theta} - \frac{EA}{2L} \int_0^L (2z'_0w' + (w')^2) dx \right) (z''_0 + w'') = 0 \quad (1)$$

completed by homogeneous boundary conditions  $w(0) = w(L) = 0$ ,  $w'(0) = w'(L) = 0$ . Here,  $E$  and  $\alpha$  are the Young's modulus and coefficient of the thermal expansion of Au, respectively,  $L$ ,  $d$ ,  $b$  are the length, width and thickness of the beam, respectively, Fig. 2(d),  $A = bd$  and  $I_{yy} = bd^3/12$  are the area and the second moment of area of the beam cross section, respectively and  $(\prime) = d/dx$ . In addition,  $\bar{\theta} = \int_0^L \theta(x) dx / L$  is the average temperature excess  $\theta(x) = T(x) - T_\infty$  above the ambient temperature  $T_\infty$ . In accordance with Eq. (1), the axial force consists of the compressive thermal force as well as the nonlinear stretching force (preserved here for generality), arising due to the axial constrain.

The initial shape  $z_0(x)$  of the beam is described by the piecewise linear function

$$z_0(x) = \frac{2h}{L}x - \frac{4h}{L}\left(x - \frac{L}{2}\right)H\left(x - \frac{L}{2}\right) \quad (2)$$

where  $h$  is the elevation of the midpoint of the beam above its ends,

Download English Version:

<https://daneshyari.com/en/article/7205888>

Download Persian Version:

<https://daneshyari.com/article/7205888>

[Daneshyari.com](https://daneshyari.com)